VOLTAGE-NOISE-INDUCED TRANSITIONS IN ELECTRICALLY EXCITABLE MEMBRANES

W. HORSTHEMKE AND R. LEFEVER *Chimie-Physique II, C.P. 231, Campus Plaine, Université Libre de Bruxelles, 1050 Bruxelles, Belgium*

ABSTRACT A quantitative study of the steady-state behavior of the sodium and potassium conductance for the Hodgkin-Huxley axon under the influence of an externally driven voltage noise is reported. The dichotomous Markov noise (random telegraph signal) considered allows for an exact evaluation of the stationary probability density of the conductances. Phase diagrams are constructed to represent the response of the system as a function of the amplitude and the correlation time of the noise. The results obtained for the Hodgkin-Huxley axon are compared with some molecular models used in the literature.

I. INTRODUCTION

Electrically excitable membrane systems, such as the giant squid axon, are among the rare biological nonequilibrium systems for which there exists a satisfactory phenomenological description of their dynamical properties. This description is based on the Hodgkin-Huxley equations (1) and accounts qualitatively and quantitatively for the changes of ionic conductance taking place during the action potential. In this paper, we investigate the behavior of this system under the influence of external voltage fluctuations. Our motivation is to describe the profound modifications of macroscopic properties that externally driven fluctuating constraints can induce. Our treatment will be based on the Hodgkin-Huxley equations.

For our purposes it is not necessary to take explicitly into account the effect of internal fluctuations in electrically excitable membranes which correspond to spontaneous events arising from the probabilistic nature of the molecular process internal to the membrane. These fluctuations have been the object of numerous studies over recent years (2–4). It is legitimate to neglect the influence of these fluctuations on macroscopic properties such as conductance and potential for areas of axon containing a large number of ionic channels. Their effect is then small, as they typically scale as one over the system size. This scaling law only breaks down in the immediate vicinity of an instability or threshold point where small spontaneous fluctuations are amplified by the dynamics of the system and drive the evolution of the macroscopic variables. This problem, namely the relation of internal fluctuations with threshold fluctuations, has been analyzed in reference 5. Note however that internal fluctuations never modify basic macroscopic features such as the location of instability and threshold points. This fact, together with the scaling law obeyed by internal fluctuations outside the immediate vicinity of instability and threshold points, insures that deterministic

---

Dr. Horsthemke's present address is the Physics Department and Institute for Fusion Studies, University of Texas, Austin, Texas 78712

phenomenological descriptions, such as the Hodgkin-Huxley model, provide a valid description of the macroscopic behavior of nonequilibrium systems.

On the other hand, the question of the behavior of ionic conductances under the influence of large, externally driven fluctuating constraints has not been dealt with up to now. In contrast to internal fluctuations, the influence of external fluctuations does not scale with an inverse power of the size of the system. Therefore, they can be of considerable importance for the behavior of macroscopic quantities even far away from instability or thresholds points. Indeed theoretical and experimental evidence obtained with physical and chemical systems indicates that in the presence of external fluctuations new behaviors and transition phenomena that are not observable in a deterministic environment become possible (6–15).

In this paper we establish that such so-called noise-induced transitions take place in the Hodgkin-Huxley system and we explore the implications of these transitions for the understanding of the molecular properties of the nerve. In this first approach we analyze separately the behavior of the sodium- and potassium-activation processes. Thus, we refer to situations in which the nerve membranes have been treated with chemical or pharmacological agents that selectively block either the sodium or the potassium channels. Experimentally this can be realized as follows: (*a*) the sodium channels are blocked by tetrodotoxin (TTX) so that only the behavior of the potassium channels is followed (16); (*b*) the potassium channels are blocked with tetraethylammonium (TEA) (17). In addition, in order to be able to disregard the interferences between the sodium activation and inactivation processes we suppose that the membrane has been treated with pronase, which inhibits inactivation (18).

The merit of these artificial situations is that they avoid getting bogged down by the full complexity of the behavior of electrically excitable membranes. It permits us to study the basic building blocks of electrical excitation separately, which is in any case essential for a subsequent interpretation of the nerve response as a whole to externally fluctuating constraints. Furthermore under the above conditions no threshold behavior is possible, regardless of the value of the potential. Thus no amplification of internal fluctuations can occur and it is safe to neglect them and to consider only those effects due to the external fluctuating constraints. Numerical simulation studies of the complete Hodgkin-Huxley system will be reported in a forthcoming paper. A further advantage of the situation we consider in this paper is that it allows for an exact analytical treatment. This is especially desirable because we deal with new kinds of transition phenomena.

We study the influence of the same externally driven constraint on sodium and potassium activation. To be specific, we consider voltage-clamp situations that realize two different values of the potential. The latter jumps between these two values at random times so that its temporal evolution corresponds to the dichotomous Markov process, also known as the random telegraph signal. Its precise definition will be stated in section II.

II. THE HODGKIN-HUXLEY AXON AND THE DICHOTOMOUS VOLTAGE NOISE

As is well known in the case of the potassium activation process, the Hodgkin-Huxley description introduces an auxiliary n variable obeying the following kinetic equation

$$\dot{n} = \alpha_4(1 - n) - \beta_4 n, \tag{1}$$

in which α_4 and β_4 are the known functions of V (in mV)

$$\alpha_4 = \frac{1}{100}(V + 10)\left[\exp\left(\frac{V}{10} + 1\right) - 1\right]^{-1}$$

$$\beta_4 = \frac{1}{8}\exp(V/80). \tag{2}$$

The potassium conductance g is then expressed in terms of the variable n by the relation

$$g = \tilde{g}_K n^4. \tag{3}$$

Setting the maximal conductance $\tilde{g}_K = 1$ the temporal evolution of the potassium conductance is given by:

$$\dot{g} = 4\alpha_4(V_t)(g^{3/4} - g) - 4\beta_4(V_t)g. \tag{4}$$

For the activation of sodium an auxiliary m variable is introduced via the kinetic equation:

$$\dot{m} = \alpha_3(1 - m) - \beta_3 m \tag{5}$$

with

$$\alpha_3 = \frac{1}{10}(V + 25)[\exp(V/10 + 5/2) - 1]^{-1}$$

$$\beta_3 = 4\exp(V/18). \tag{6}$$

Since the inactivation process is disregarded in the situations considered here, the sodium conductance is a function of m only, $g = \tilde{g}_{Na}\, m^3$, and its temporal evolution is given by Eq. 7. (Maximal sodium conductance has been normalized to one).

$$\dot{g} = 3\alpha_3(V_t)(g^{2/3} - g) - 3\beta_3(V_t)g. \tag{7}$$

In summary, sodium and potassium conductances obey here an equation of the general form:

$$\dot{g} = \nu\alpha_\nu(V_t)[g^{(\nu-1)/\nu} - g] - \nu\beta_\nu(V_t)g \equiv F(g, V_t) \tag{8}$$

with $\nu = 4$ for K^+ and $\nu = 3$ for Na^+.

Below we will analyze the behaviour of these conductances for the case in which V_t is a random process fluctuating between two well-defined values:

$$V_t = V + I_t. \tag{9}$$

I_t is the dichotomous Markov process (19, 20), whose state space consists only of two levels $\{-\Delta, \Delta\}$.

Since I_t is a Markov process, it is entirely characterized by its transition probabilities $P_\pm(t\,|\,I_0) = P(I_t = \pm\Delta\,|\,I_0)$, i.e. the probabilities that the process takes the values $\pm\Delta$ at time t given that it was in the state I_0 at time t_0 ($t \geq t_0$). The temporal evolution of these transition probabilities is given by the master equation:

$$\frac{d}{dt}\begin{bmatrix} P_+(t\,|\,I_0) \\ P_-(t\,|\,I_0) \end{bmatrix} = -\frac{\gamma}{2}\begin{bmatrix} 1 & -1 \\ -1 & 1 \end{bmatrix}\begin{bmatrix} P_+(t\,|\,I_0) \\ P_-(t\,|\,I_0) \end{bmatrix}, \tag{10}$$

where $\gamma/2$ is the mean frequency of transition from one state to the other. If I_t is started with equal probability for both states, I_t is a stationary process with mean value zero;

$$E\{I_t\} = 0, \tag{11}$$

correlation function

$$E\{I_t I_{t'}\} = \Delta^2 e^{-\gamma|t-t'|} \tag{12}$$

and correlation time

$$\tau_{cor} = \gamma^{-1}. \tag{13}$$

The spectral density of I_t is of course given by a Lorentzian

$$S(f) = \frac{\gamma\Delta^2}{\pi(f^2 + \gamma^2)}. \tag{14}$$

The stationary behavior of the K^+ and Na^+ conductance can be determined exactly. Indeed as is derived in the appendix (see also 21)[1], the stationary probability density $P_s(g)$ is given by:

$$P_s(g) = N\left[\frac{1}{F(g, V+\Delta)} - \frac{1}{F(g, V-\Delta)}\right] \cdot \exp\left\{-\frac{\gamma}{2}\int^g dg'\left[\frac{1}{F(g', V+\Delta)} + \frac{1}{F(g', V-\Delta)}\right]\right\} \tag{15}$$

where N is the normalization constant. $P_s(g)$ is defined on the interval

$$U = [g_s(V-\Delta), g_s(V+\Delta)] \tag{16}$$

which is called the support of $P_s(g)$. Here $g_s(V \pm \Delta)$ denotes the steady-state solution of Eq. 8 corresponding to the value $V \pm \Delta$ of the potential. The significance of the support is explained in Fig. 1 and it is easily seen that $P_s(g)$ necessarily vanishes identically outside U.

The local extrema of the stationary probability density $P_s(g)$ (see Appendix) are the zeroes of

$$-\left[F'(g, V+\Delta) + \frac{\gamma}{2}\right] \cdot F^2(g, V-\Delta) + \left[F'(g, V-\Delta) + \frac{\gamma}{2}\right] \cdot F^2(g, V+\Delta) = 0$$

$$F' \equiv \frac{\partial F(g, V)}{\partial g}. \tag{17}$$

They are of special interest for two reasons. First, the number and location of the extrema contain some valuable information about the shape of the probability density and therefore,

[1]Kitahara K., W. Horsthemke, R. Lefever, and Y. Inaba. 1980. Phase diagrams of noise induced transitions. Exact results for a class of external coloured noise. *Prog. Theoret. Phys.* 64:1233–1247.

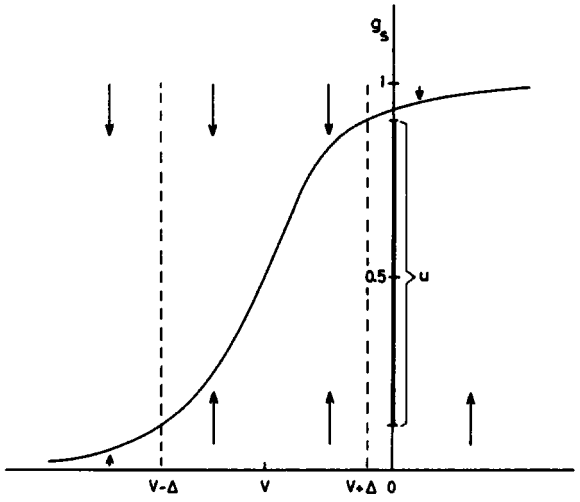

FIGURE 1 Schematic plot of the curve of the deterministic steady states of Eq. 1 as a function of V. The state space of the random process (g_t, V_t) is given by two broken lines at $V \pm \Delta$. The arrows indicate the direction of the evolution of g_t. It is obvious that the whole probability mass will be inside the support U, indicated by the bold face line on the g_s-axis, for $t \to \infty$.

about the stationary behaviour of the conductance g_t. Second, the system we consider is ergodic under the influence of dichotomous noise. This means that the stationary probability density $P_s(g)$ is equal to the fraction of time that anyone of the realizations of the process g_t spends in an infinitesimal neighbourhood of the value g. This leads us to identify the extrema with the macroscopic steady states: the maxima, the most probable states where the process spends, relatively, a lot of time with stable macroscopic steady states; the minima, which the process leaves quickly, with unstable macroscopic steady states.

The probability density $P_s(g)$ can always be normalized. As far as its behavior near the boundaries of the support is concerned however, it can change from divergent to nondivergent. It is easily verified that the probability density diverges at the boundaries when the inverse of the correlation time γ satisfies the following condition (see Appendix):

$$-2F'(g_s(V \pm \Delta), V \pm \Delta) > \gamma_{\pm}. \tag{18}$$

γ_+ refers to the conditions for the upper boundary, γ_- for the lower boundary. When Eq. 18 is not fulfilled, $P_s(g)$ vanishes at the boundary. On the basis of these formulae, a complete picture of the steady-state properties of the Hodgkin-Huxley axon under fluctuating voltage-clamp conditions can be obtained and is reported in the next section.

III. PHASE DIAGRAMS FOR THE SODIUM AND POTASSIUM CONDUCTANCE OF THE HODGKIN AND HUXLEY AXON

Using the expression for $F(g, V \pm \Delta)$ given in Eq. 8, and Eqs. 2 and 3 for α and β, the potassium and sodium stationary probability density can be calculated directly from Eq. 15. In the potassium case, it reads (for simplicity of notations the subscript 4 on α and β has been

dropped):

$$P_s(g) = Ng^{-3/4}\{\alpha(V-\Delta) - \alpha(V+\Delta) + [\alpha(V-\Delta) + \beta(V-\Delta) - \alpha(V+\Delta) - \beta(V+\Delta)]g^{1/4}\} \cdot |\alpha(V+\Delta) - [\alpha(V+\Delta) + \beta(V+\Delta)]g^{1/4}|^{\{(\gamma/2)[\alpha(V+\Delta)+\beta(V+\Delta)]\}-1} \cdot |\alpha(V-\Delta) - [\alpha(V-\Delta) + \beta(V-\Delta)]g^{1/4}|^{\{(\gamma/2)[\alpha(V-\Delta)+\beta(V-\Delta)]\}-1}. \quad (19)$$

Its extrema are given by:

$$-\left[\alpha(V+\Delta)\left(\frac{3}{4}-n\right) - \beta(V+\Delta)n + \frac{\gamma}{2}n\right] \cdot [\alpha(V-\Delta)(1-n) - \beta(V-\Delta)n]^2 + \left[\alpha(V-\Delta)\left(\frac{3}{4}-n\right) - \beta(V-\Delta)n + \frac{\gamma}{2}n\right] \cdot [\alpha(V+\Delta)(1-n) - \beta(V+\Delta)n]^2 = 0, n = g^{1/4}. \quad (20)$$

(See Eq. 17). The stationary probability density diverges at the lower boundary of the support U when

$$\gamma_+ = 2[\alpha(V+\Delta) + \beta(V+\Delta)] \quad (21)$$

and at the upper boundary when

$$\gamma_- = 2[\alpha(V-\Delta) + \beta(V-\Delta)]. \quad (22)$$

In a similar way, corresponding expressions for the sodium system can directly be obtained.

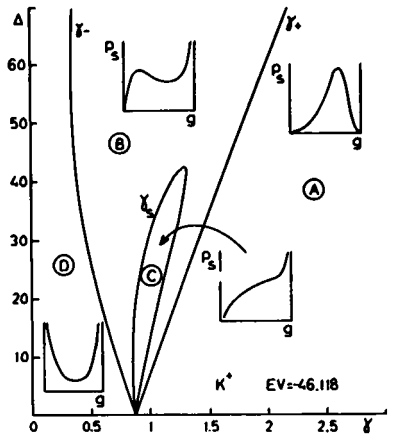

FIGURE 2a

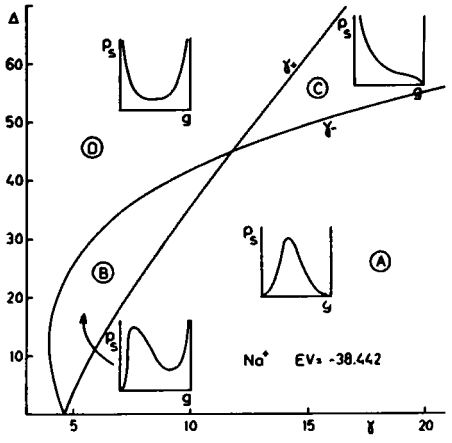

FIGURE 2b

FIGURE 2 (*a*) Phase diagram of the potassium system as a function of the amplitude Δ and the inverse of the correlation time γ. The value chosen for the average potential is −46.1 mV; it corresponds to $g_K = 1/2$ under deterministic conditions. On the line γ_+ (γ_-) the behavior of the probability density P_s near the upper (lower) boundary of the support U changes abruptly from nondivergent to divergent. γ_s is the line on which the minimum and maximum existing in domain B coalesce. (*b*) Phase diagram of the sodium system as a function of the amplitude Δ and the inverse of the correlation time γ. The value chosen for the average potential is −38.4 m; it corresponds to $g_{Na} = 1/2$ under deterministic conditions. The lines γ_+, γ_- have the same meaning as in Fig. 2(*a*).

Using these expressions, phase diagrams can be constructed that display in a concise way the response of conductances to external voltage fluctuations of amplitude Δ and correlation time γ^{-1} (see Fig. 2). For both the potassium and sodium the mean value of the applied potential corresponds to $g = 1/2$ under deterministic conditions; i.e., $E\{V_t\} = -46.1\text{mV}$ for the potassium and $E\{V_t\} = -38.4\text{mV}$ for the sodium.

Fig. 2*a* reports the results for the potassium system. For a given value of Δ, the probability density diverges at the upper (lower) boundary of the support U, if γ is chosen to the left of γ_+ (γ_-). This accounts for the existence of regions A and D in which the probability exhibits only one extremum. In region A, the extremum is a maximum, in D it is a minimum. If the value of Δ is chosen above 42.5 mV, and γ increases from zero and crosses the γ_- line, $P_s[g_s(V \pm \Delta)]$ vanishes and thus the probability distribution acquires an additional extremum (which of course is a maximum). When it crosses the γ_+ line the disappearance of the divergence at the upper boundary of U leads to the disappearance of the minimum. Below 42.5 mV, the probability density has a saddle point for $\gamma = \gamma_s$ at which the minimum and maximum of region B coalesce. As a result, inside γ_s one has a domain C in which the probability density is monotonously increasing from the lower to the upper boundary of the support. Fig. 3 represents the typical behavior of the probability density $P_s(g)$ for each of these regions. The influence of the correlation time on the location of the extrema is given in Fig. 4, for two typical values of the density of the external noise: one is chosen below the threshold value $\Delta \simeq 42.5\text{mV}$ and the other one is chosen above this value. Below, provided γ is not taken in region C, there is always an extremum in the neighbourhood of $g = 0.5$. This extremum is a

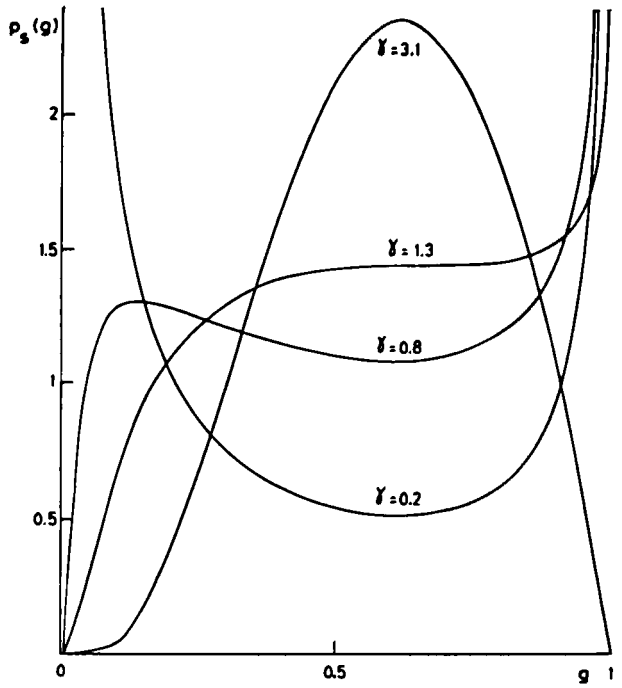

FIGURE 3 Probability density of the potassium system for values of γ chosen in regions A ($\gamma = 3.1$), B ($\gamma = 0.8$), C ($\gamma = 1.3$), D ($\gamma = 0.2$) of Fig. 2*a* and Δ equal to 40 mV. The support $U = (2.94 \times 10^{-2}, 0.804)$ corresponding to the value chosen for Δ has been uniformly stretched to (0, 1).

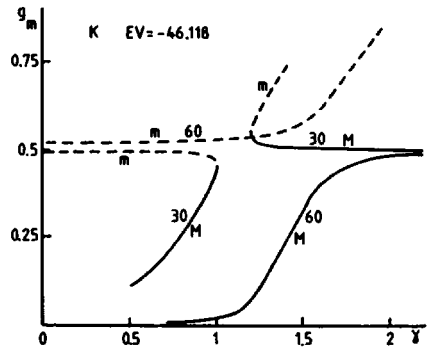

FIGURE 4 The location g_m of the extrema of $P_s(g)$ for the potassium system is displayed as a function of γ for Δ = 60 mV and Δ = 30 mV. The minima (m) are indicated in broken line and the maxima (M) in solid line.

minimum to the left of region C and a maximum to the right of C. The location of the second extremum, which exists in region B, increases rapidly with γ from values that lie near the lower boundary of the support to values near the upper boundary. Above Δ = 42.5mV, the minimum, which starts out near g = 0.5, for small values of γ, moves rapidly to the upper boundary, which it attains at $\gamma = \gamma_+$. The maximum, which appears at $\gamma = \gamma_-$, approaches g = 0.5 when $\gamma \rightarrow \infty$.

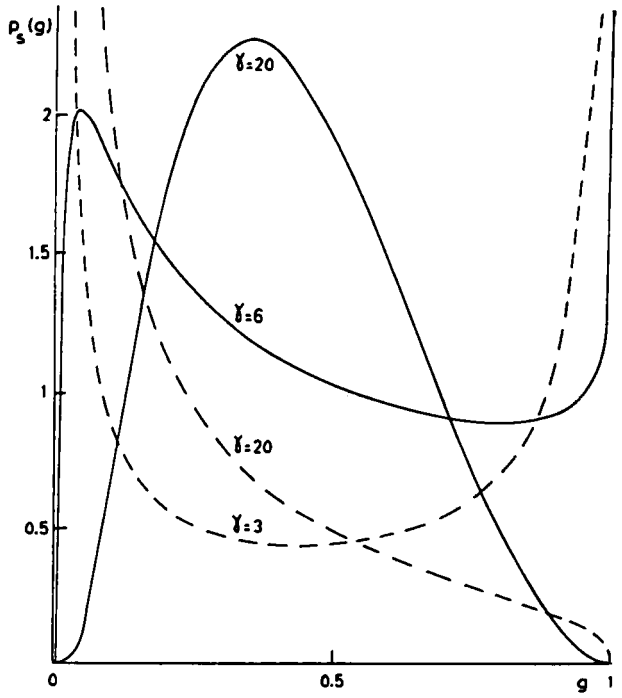

FIGURE 5 Probability density of the sodium system for values of the parameters as indicated in the figure. Broken lines, Δ = 60 mV, solid lines, Δ = 20 mV. The support U = (3.599 × 10^{-2}, 0.876) for Δ = 20 mV and U = (3.798 × 10^{-8}, 0.933) for Δ = 60 mV has been stretched uniformly to (0, 1).

In Fig. 2*b* we report the results for the sodium system. Since the characteristic time of the sodium channels is much shorter than for the potassium system, as can be seen from the coefficients α_v and β_v, the region of interest is shifted to higher values of γ, i.e., to shorter correlation times. Remarkably, in spite of the fact that the sodium and potassium activation obey equations that are very similar, differing only in the power ν of the auxiliary variable, there is an essential difference in their phase diagrams. This is basically due to the fact that for the sodium system the γ_+ and γ_- curves cross each other for a value of the depolarization that remains physiologically acceptable. This has the following three consequences: (*a*) contrary to what happens in the K^+ system, the domain *C* where $P_s(g)$ is a monotonous function is restricted to the value of $\Delta > \sim 45$mV; (*b*) the divergence occurs at the lower boundary of the support, whereas for the potassium case it is at the upper boundary; (*c*) the region *B*, where two extrema occur, now occupies a finite domain in the (Δ, γ) plane. The behavior of the probability density in each of these regions is displayed in Fig. 5. Though the behavior of the probability density in region *C* is qualitatively identical in both systems it is important to emphasize that the mechanism of transition to this region is basically different in the sodium and potassium system: in the case of the potassium system, one deals with a soft transition corresponding to a local event inside the support, namely the coalescence of two extrema into a saddle point. This phenomenon does not affect the behavior of the probability density near the boundaries of the support. This aspect ties it in with the noise-induced phase transitions of the peak splitting type described elsewhere.[1] In contrast, in the sodium system region *C* appears via a hard transition caused by the abrupt change of behavior at one of the boundaries of the support.

The marked difference between the potassium and the sodium channels is further illustrated in Fig. 6, which gives the location of the extrema of $P_s(g)$ as a function of γ for Δ fixed. Whatever the value of Δ, for small γ, there is always a minimum near $g = 0.5$. It moves towards the upper boundary of the support which it attains for $\gamma = \gamma_+$. For $\gamma \geq \gamma_-$ the location of the additional extremum of $P_s(g)$ (maximum), which appears at the lower boundary,

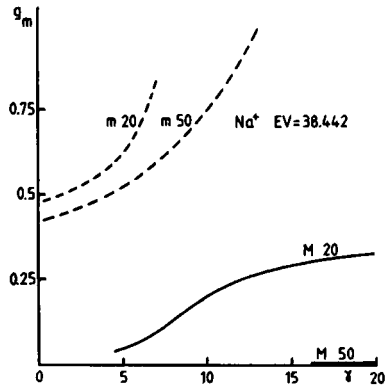

FIGURE 6 The location g_m of the extrema of $P_s(g)$ for the sodium system is displayed as a function of γ for $\Delta = 20$ mV and $\Delta = 50$ mV. For $\Delta = 50$ mV, the unique extremum in region *D* (cf. Fig. 2*b*) coincides, for the values of γ reported, almost with the lower boundary of *U*. However, for γ tending to infinity it will approach the deterministic steady state $g = 0.5$. The broken lines correspond to minima (m) and the solid lines to maxima (M).

increases slowly towards $g = 0.5$. The greater the intensity of the noise, the slower is the rate of approach to $g = 0.5$. As is to be expected from the phase diagram, the two curves overlap only if $\Delta < 45$mV. The results of this section are a good illustration of the fact that systems, the deterministic phenomenological description of which closely resemble each other, can respond to externally fluctuating constraints in quite different ways.

IV. SOME EXAMPLES OF MOLECULAR MODELS AND THE INFLUENCE OF VOLTAGE NOISE

In this section, the behavior of some simple models, based on the molecular properties of nerve membranes under fluctuating external constraints, is briefly compared with our predictions for the Hodgkin-Huxley axon. These models start from the experimental fact that single channels are two-state systems (open-closed) (3, 4, 22–24). Their general drawback is that the fit with the experimental data is in most cases not as perfect as the Hodgkin-Huxley equations. The simplest model of this kind that has been studied in the literature (23) leads to the following kinetic equation:

$$\dot{g} = k_c(1 - g) - k_0 g. \tag{23}$$

In this equation g is the fraction of open channels and can be directly identified with the conductance of the nerve membrane if g_{max} is again normalized to one. For the potential dependence of the rate constants k_c and k_0 the following form can be assumed:

$$\begin{aligned} k_c &= f_c \exp(\mu V) \\ k_0 &= f_0 \exp(-\mu V). \end{aligned} \tag{24}$$

This form is especially appropriate in the case of a gating mechanism involving the reorientation of dipoles in the membrane (25). Dependence of the rate constants k_c and k_0 involving higher orders of V in the exponential function have been considered in references 26 and 27. The steady state of Eq. 23 is of course given by

$$g_s = \{1 + \exp[2\mu(V' - V)]\}^{-1} \tag{25}$$

where $V' \equiv 1/2\mu \ln f_0/f_c$. Hence, g_s equals one half for V equal to V'.

As for the Hodgkin-Huxley axon we now assume that the potential V_t fluctuates around the mean value $E\{V_t\} = V'$ as the dichotomous Markov process described in section II. Straightforward calculations yield for the equation of the extrema g_m of $P_s(g)$ in this case the following form:

$$\left[-2e^{\mu V'} \cosh(\mu\Delta) + \frac{\gamma}{2f_c}\right] \cdot [-4g_m \sinh(2\mu\Delta) + 2\sinh(2\mu\Delta)] = 0. \tag{26}$$

As is easily seen the second factor vanishes for $g_m = 1/2$, independently of the intensity Δ and the correlation time γ^{-1}. This is the unique local extremum of $P_s(g)$ which is symmetrical around this value. If the first factor vanishes, there is the following relation between Δ and γ:

$$\gamma = 4f_c e^{\mu V'} \cosh(\mu\Delta), \tag{27}$$

and $P_s(g) \equiv$ constant on the support U. It is easily verified that the γ given by Eq. 27

coincides with the values $\gamma_\pm$ (cf. 18). As a result, the phase diagram for this two state model, Eq. 23, is extremely simple: it consists of two regions, of the type *A* and *D* of Fig. 2, the transition from one domain to the other occurs on the line given by Eq. 27.

The question of the existence of cooperative interactions in excitable membranes has often been raised in the literature (28–31). In the case of electrically excitable membranes, the influence of cooperativity in a two-state model can be taken into account as follows:

$$\dot{g} = f_c e^{\mu V}(1 - g)e^{\eta g^2} - f_0 e^{-\mu V} g e^{\eta(1-g)^2}$$

$$[f_0 = f_c \exp(2\mu V') \text{ (as in Eq. 24)}]. \tag{28}$$

if cooperativity is supposed to act in a completely symmetric way, or

$$\dot{g} = f_c e^{\mu V}(1 - g) - f_0 e^{-\mu V} g e^{\eta g} \tag{29}$$

for the assymmetric case in which cooperativity systematically favors the open state. Again the mean value of the dichotomous voltage noise was chosen such that under the deterministic conditions it corresponds to $g_s(V) = \frac{1}{2}$. Furthermore, f_c was adjusted so that the time scale of Eqs. 28 and 29 is identical to that of the potassium system of the Hodgkin-Huxley axon. The value of μ has been chosen so as to give a good fit of the steady-state conductance of the K^+ system. As for the Hodgkin-Huxley axon in section III, the phase diagrams for these cooperative two-state models were constructed. The results reported in Figs. 7 and 8 show clearly that the nonlinearity that results from the cooperativity leads to a richer behavior in a fluctuating environment than Eq. 23. Furthermore it can be seen that the symmetry properties of the cooperativity are reflected in the phase diagrams. It is striking that neither phase diagram of the molecular models considered in this section bears any close resemblance to that of the potassium conductance of the Hodgkin-Huxley axon. This is particularly remarkable since under deterministic conditions all the models yield a satisfactory fit of the steady-state voltage-clamp data.

V. CONCLUSION

Let us now come back to the main subject of our analysis, namely the behavior of the Hodgkin-Huxley axon submitted to an externally driven voltage noise. The results obtained in section III show some features that are quite interesting from a physiological point of view: (*a*) in the deterministic situation there is no threshold behavior in the dynamics of the sodium and potassium conductance under the conditions considered above. Nevertheless the domain *C* and the threshold of the complete Hodgkin-Huxley system seem to be related. Indeed, the lower boundary of this domain in the sodium case, and the upper boundary in the potassium case, typically correspond to values on the order of 40 mV. (*b*) As far as the regions where the probability density diverges only at one boundary of the support are concerned, the potassium and sodium systems behave in the same way below this "threshold" Δ, i.e., both channels are preferentially in the open state. In contrast, above this threshold Δ, the behavior of the sodium system changes in the sense that now *it favors the closed state*. This is a strong indication that external fluctuations on the complete Hodgkin-Huxley system could lead to a shift of the threshold value, a phenomena that, in the case of chemical system, has already been described in detail theoretically (7, 8, 10) and has been observed experimentally (14, 15). From a

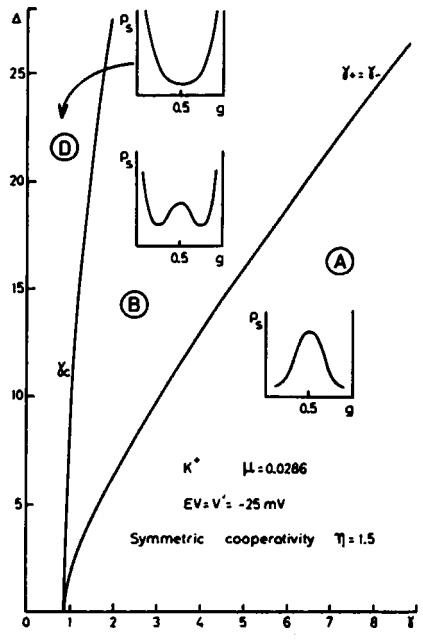

FIGURE 7

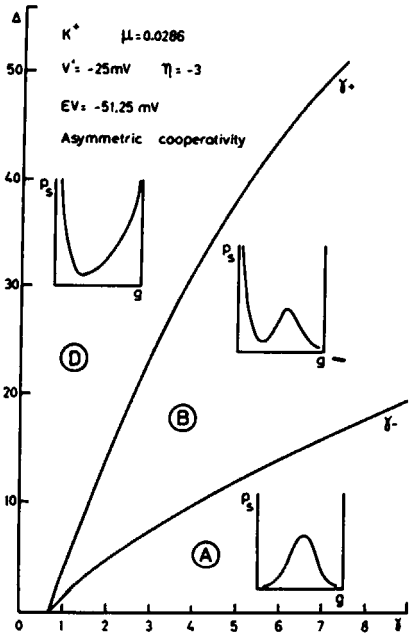

FIGURE 8

FIGURE 7 Phase diagram of model Eq. 16 in terms of Δ and γ. The typical behavior of $P_s(g)$ is sketched for the different regions. The line γ_c is the location of the critical points where the maximum and the two minima of region B coalesce. The cooperativity constant η has been chosen such that under deterministic conditions no bistability occurs. Deterministically bistable behavior is only possible for $\eta \geq 2$. The probability density changes from nondivergent to divergent at the boundaries on the lines γ_+ and γ_-, which coincide in this model.

FIGURE 8 Phase diagram of model Eq. 17 in terms of Δ and γ. The typical behavior of $P_s(g)$ is sketched for the different regions for $\eta = -3$. For $\eta > 0$, the line γ_- lies above γ_+ and hence in region B divergence occurs at the upper boundary instead of the lower one. Under deterministic conditions bistability occurs only for $\eta \leq -4$. Hence the relative distance to the deterministic critical point is the same as in Fig. 7.

fundamental point of view this also raises the interesting question of whether, in the vicinity of this new threshold point, the internal fluctuations would have the same behavior as in reference 5. (*c*) Compared with other biologically relevant systems that also have no instability under deterministic environmental conditions (32)[1] the phase diagram of the nerve system (Fig. 2) is less complex. This suggests that the nerve system is less sensitive to the influence of external noise. Interestingly, the same result holds for the molecular models considered in section IV.

As for the more general framework of nonequilibrium systems, the theoretical results obtained in this paper show clearly that the Hodgkin-Huxley axon belongs to the class of nonlinear systems whose stationary state behavior can be deeply modified by external fluctuations. Indeed, under the conditions specified in the introduction, both the sodium and the potassium conductance of the nerve membrane can undergo noise-induced transitions in the phenomenological Hodgkin-Huxley description: the shape of the probability density changes drastically at certain well-defined values of the amplitude and correlation time of the

external fluctuations. The particular significance of this phenomenon lies in the fact that the Hodgkin-Huxley equations represent a good quantitative description of the experimental behavior of nerve-membrane conductances under deterministic environmental conditions, e.g. the usual voltage-clamp conditions. Thus we may consider that the starting point of our analysis of the influence of external voltage noise is reliable and that experimental confirmation should be possible. We believe that an experimental observation of the predicted phenomena is feasible because (*a*) dichotomous Markov noise is not difficult to generate electronically. (*b*) The typical switching time for voltage-clamp experiments is microseconds whereas the typical time scale of the conductances is 1–10 ms, so that the correlation time of the noise can range over a sufficiently large interval (down to one tenth, or less, of the characteristic time of the conductances). (*c*) Since the interesting range of correlation times is shorter or of the order of the typical duration of an action potential, the mean frequency γ is high enough that the experiments can be carried out over a sufficiently long time to obtain reliable conductance statistics. To directly compare our theoretical predictions with experimental results, it is necessary to disregard in the current measurements the capacitive currents that follow each jump of the potential. It is also known that nerve membranes have a leakage current which was not explicitely taken into account in our analysis. This is justified since the leakage conductance is not voltage dependent. This has the consequence that the leakage current takes only two well-defined values corresponding to the values $V \pm \Delta$ of the potential. The currents measured under fluctuating potential conditions can thus be corrected by subtracting the leakage component corresponding to the actual value of the potential.

Furthermore, comparing the results of section IV with those of section III, we explicitly stress the fact that different kinetic schemes that agree reasonably well with each other under deterministic environmental conditions, lead to markedly different predictions for the behavior of the system under fluctuating constraints. Hence any essential deviations in kinetics of real nerve membranes from the Hodgkin-Huxley axon would be clearly revealed in a fluctuating environment. This is, of course, a very nice feature for confirming or rejecting the theoretical predictions of section III. Furthermore this demonstrates that probing the nerve membrane behavior with external dichotomous noise should be a convenient method for exploring its molecular properties and discriminating between different kinetic descriptions.

In summary, an experimental study of the influence of external voltage noise on the sodium and potassium conductance of nerve membranes is worthwhile for two main reasons: (*a*) the system is ideally suited for the experimental observation of the new phenomenon of noise-induced transitions since it does not have the same drawbacks as the physicochemical systems that have been used so far for this purpose. The results reported in (11–13) are essentially analog simulations, whereas in references 14 and 15, a chemical system was studied in which the kinetic mechanism is only known in a rather limited way and hence no precise quantitative description is available. (*b*) It allows us to test the validity of the phenomenological Hodgkin-Huxley description outside its classic range of application. The main advantage of studying the response of the nerve to a stochastic voltage clamp as compared to a deterministic one, is that this procedure generates in a simple manner a signal with a broad-band frequency spectrum. Obviously the more frequencies that are contained in the input, the more details of the dynamics of the system will be revealed. The phase diagrams are an economical way to discriminate between different dynamic systems.

APPENDIX

We will present below a detailed derivation of Eq. 15 for the stationary probability density, of Eq. 17 for its extrema; as well as the condition for divergence at the boundaries Eq. 18.

Let I_T be the dichotomous Markov process as defined in section II. Consider a system whose state is described by the following stochastic differential equation

$$\dot{x}_t = F(x_t, I_t), \tag{A1}$$

where F can be nonlinear in both variables. Because I_t is by definition Markovian and because the temporal evolution of x is given by a first-order differential equation, it is obvious that the composite process (x_t, I_t) is Markovian: the knowledge of the actual state of this composite process at some time t_0 is totally sufficient to predict its future stochastic evolution for $t > t_0$. Note that the first component, x_t, taken by itself is not a Markov process. Because of the particular structure of the composite process (i.e., the second component, I_t, is not influenced by the first) it is intuitively clear that the evolution equation for the joint probability $P(x, I, t)$ consists of two parts: one describes the evolution of x_t for a fixed value of the dichotomous noise, i.e. $I_t = \Delta$ or $I_t = -\Delta$, and one governs the evolution of the dichotomous Markov noise, which is given by the Master equation (10). Hence we have:

$$\begin{aligned} \partial_t P(x, \Delta, t) &= -\partial_x F(x, \Delta) P(x, \Delta, t) - \frac{1}{2}\gamma q(x, t) \\ \partial_t P(x, -\Delta, t) &= -\partial_x F(x, -\Delta) P(x, -\Delta, t) + \frac{1}{2}\gamma q(x, t), \end{aligned} \tag{A2}$$

where $q(x, t) \equiv P(x, \Delta, t) - P(x, -\Delta, t)$.

This evolution equation can be rigorously derived by starting from the Chapman-Kolmogorov equation for the pair process (x_t, I_t) and evaluating the transition probabilities of this Markov process $P(x, I, t + h | y, J, t)$ for infinitesimally small h as explained in reference 21.[1] For the stationary joint probability $P_s(x, I)$ we have

$$0 = -\partial_x F(x, \Delta) P_s(x, \Delta) - \frac{1}{2}\gamma q_s(x) \tag{A3a}$$

$$0 = -\partial_x F(x, -\Delta) P_s(x, -\Delta) + \frac{1}{2}\gamma q_s(x). \tag{A3b}$$

Adding the two equations, we obtain:

$$0 = -\partial_x [F(x, \Delta) P_s(x, \Delta) + F(x, -\Delta) P_s(x, -\Delta)], \tag{A4a}$$

and subtracting them:

$$0 = -\partial_x [F(x, \Delta) P_s(x, \Delta) - F(x, -\Delta) P_s(x, -\Delta)] - \gamma q_s(x). \tag{A4b}$$

The quantity that really interests us, however, is not the joint stationary probability, but the stationary probability density $P_s(x)$ for the first component only. It is obtained by summing up the states of the random telegraph signal, i.e.,

$$P_s(x) = P_s(x, \Delta) + P_s(x, -\Delta). \tag{A5}$$

It is now convenient to write the right-hand side of the differential eq. A1 as a sum of two terms, namely one even with respect to the second variable $F_e(x, -\Delta) = F_e(x, \Delta)$ and the other one odd $F_o(x, -\Delta) = -F_o(x, \Delta)$:

$$F(x, \Delta) = F_e(x, \Delta) + F_o(x, \Delta) \tag{A6a}$$

$$F(x, -\Delta) = F_e(x, -\Delta) + F_o(x, -\Delta)$$
$$= F_e(x, \Delta) - F_o(x, \Delta). \tag{A6b}$$

Of course $F_e(x, \Delta) = \frac{1}{2}F(x, \Delta) + \frac{1}{2}F(x, -\Delta)$ and $F_o(x, \Delta) = \frac{1}{2}F(x, \Delta) - \frac{1}{2}F(x, -\Delta)$.

Thus we can write Eq. A4*a* as

$$0 = -\partial_x[F_e(x, \Delta)P_s(x, \Delta) + F_o(x, \Delta)P_s(x, \Delta)$$
$$+ F_e(x, \Delta)P_s(x, -\Delta) - F_o(x, \Delta)P_s(x, \Delta)]$$
$$= -\partial_x[F_e(x, \Delta)P_s(x) + F_o(x, \Delta)q_s(x)]. \tag{A7a}$$

In a similar way we obtain for (A4*b*):

$$0 = -\partial_x[F_e(x, \Delta)q_s(x) + F_o(x, \Delta)P_s(x)] - \gamma q_s(x). \tag{A7b}$$

Hence we can conclude

$$F_e(x, \Delta)P_s(x) + F_o(x, \Delta)q_s(x) = \text{constant}. \tag{A8}$$

This constant has to be equal to zero, since

$$P_s(x, \Delta) = P_s(x, -\Delta) \equiv 0 \tag{A9}$$

if x is not in the interval $U = [x_s(-\Delta), x_s(\Delta)]$. $x_s(\pm\Delta)$ is defined by $F(x_s(\pm\Delta), \pm\Delta) = 0$. The significance of this support U has been explained in section II and Fig. 1. From (A8) with constant = 0

$$q_s(x) = -\frac{F_e(x, \Delta)}{F_o(x, \Delta)}P_s(x) \tag{A10}$$

and

$$\partial_x q_s(x) = q_s'(x) = \left[-\frac{F_e'(x, \Delta)}{F_o(x, \Delta)} + \frac{F_e(x, \Delta)F_o'(x, \Delta)}{F_o^2(x, \Delta)}\right]P_s(x) - \frac{F_e(x, \Delta)}{F_o(x, \Delta)}P_s'(x). \tag{A11}$$

Expressing $q_s(x)$ and $q_s'(x)$ in (A7*b*) in terms of $P_s(x)$ and $P_s'(x)$ with the help of the Eqs. A10 and A11, we obtain after some ordering $[F_e = F_e(x, \Delta), F_o = F_o(x, \Delta)]$

$$\left(\frac{F_o^2 - F_e^2}{F_o}\right)P_s'(x) = \frac{F_oF_e(F_e' + \gamma) + F_oF_eF_e' - F_e^2F_o' - F_o^2F_o'}{F_o^2}P_s(x) \tag{A12}$$

or

$$P_s'(x) = \left[\frac{\gamma F_e}{F_o^2 - F_e^2} + \frac{F_o(2F_eF_e' - F_oF_o') - F_e^2F_o'}{F_o(F_o^2 - F_e^2)}\right]P_s(x). \tag{A13}$$

Using the definitions of F_e and F_o it is easily verified that

$$\frac{\gamma F_e}{F_o^2 - F_e^2} = -\frac{\gamma}{2}\left[\frac{1}{F(x, \Delta)} + \frac{1}{F(x, -\Delta)}\right] \tag{A14}$$

and

$$\frac{F_o(2F_eF_e' - F_oF_o') - F_e^2F_o'}{F_o(F_o^2 - F_e^2)} = \partial_x \ln\left[\frac{1}{F(x, \Delta)} - \frac{1}{F(x, -\Delta)}\right]. \tag{A15}$$

Hence we obtain for the stationary probability density

$$P_s(x) = N\left[\frac{1}{F(x,\Delta)} - \frac{1}{F(x,-\Delta)}\right] \cdot \exp\left\{-\frac{\gamma}{2}\int^x \left[\frac{1}{F(x',\Delta)} + \frac{1}{F(x',-\Delta)}\right] dx'\right\}, \quad \text{(A16)}$$

where N is the normalization constant

$$\int_{x_s(-\Delta)}^{x_s(\Delta)} P_s(x')\,dx' = 1. \quad \text{(A17)}$$

The extrema of the stationary probability density $P_s(x)$ are determined by the condition

$$\partial_x P_s(x)\,|_{x_m} = 0. \quad \text{(A18)}$$

From Eq. A16, we obtain,

$$\left[-\frac{F'(x_m,\Delta)}{F^2(x_m,\Delta)} + \frac{F'(x_m,-\Delta)}{F^2(x_m,-\Delta)} - \frac{\gamma}{2F^2(x_m,\Delta)} + \frac{\gamma}{2F^2(x_m,-\Delta)}\right] \cdot N\exp\left\{-\frac{\gamma}{2}\int^{x_m}\left[\frac{1}{F(x',\Delta)} + \frac{1}{F(x',-\Delta)}\right]dx'\right\} = 0. \quad \text{(A19)}$$

Since in the interior of the support U, $F(x,\Delta) \neq 0$ and $F(x,-\Delta) \neq 0$, (A19) reduces to the condition:

$$-\left[F'(x_m,\Delta) + \frac{\gamma}{2}F^2(x_m,-\Delta) + F'(x_m,-\Delta) + \frac{\gamma}{2}\right]F^2(x_m,\Delta) = 0 \quad \text{(A20)}$$

Let us now consider the behavior of $P_s(x)$ near the boundaries of the support N. Choosing the lower one $x_s(-\Delta)$, [the calculations for $x_s(\Delta)$ are completely analogous], we write for x near this boundary:

$$x = x_s(-\Delta) + \delta x \quad \text{(A21)}$$

Under the condition that $F(x_s(-\Delta), +\Delta) \neq 0$, $P_s(x)$ in the vicinity of $x_s(-\Delta)$ can be written as, by making a Taylor expansion of $F(x, \pm\Delta)$ around $x_s(-\Delta)$:

$$P_s(x) \sim \frac{1}{F'(x_s(-\Delta),-\Delta)\delta x}\exp\left[-\frac{\gamma}{2}\int^{\delta x} d\delta x\,\frac{1}{F'(x_s(-\Delta),-\Delta)\delta x}\right]. \quad \text{(A22)}$$

Hence, we have

$$P_s(x) \sim |\delta x|^{-\gamma/2F'(x_s(-\Delta),-\Delta)-1} \quad \text{(A23)}$$

near $x_s(-\Delta)$ and similarly,

$$P_s(x) \sim |\delta x|^{-\gamma/2F'(x_s(\Delta),\Delta)-1} \quad \text{(A24)}$$

near $x_s(\Delta)$. This shows that $P_s(x)$ is always normalizable for a deterministically stable system, i.e., $F'(x_s(\pm\Delta), \pm\Delta) < 0$, since in this case, we always have

$$-\frac{\gamma}{2F'(x_s(\pm\Delta),\pm\Delta)} > 0. \quad \text{(A25)}$$

The stationary density diverges at the upper boundary, in an integrable way as follows from Eq. A25, if

$$-\frac{\gamma}{2F'(x_s(\Delta),\Delta)} - 1 < 0 \quad \text{(A26)}$$

and at the lower boundary, if

$$-\frac{\gamma}{2F'(x_s(-\Delta), -\Delta)} - 1 < 0. \tag{A27}$$

Early stages of this study were done in collaboration with Dr. D. van Lamsweerde-Gallez from the University of Brussels. We benefited very much from the numerous stimulating and interesting discussions we had with her. We also thank Professors A. A. Verveen, J. De Goede, and R. J. van den Berg from the University of Leiden and Professor B. Neumcke of the University of Saarbrücken for critical discussions and helpful comments.

This work was supported by the Instituts Internationaux de Physique et de Chimie fondés par E. Solvay and by the Belgian Government: Actions de Recherche Concertées, convention n° 76.81II.3.

Received for publication 2 March 1980 and in revised form 20 November 1980.

REFERENCES

1. Hodgkin, A. L., and A. F. Huxley. 1952. Currents carried by sodium and potassium ions through the membrane of the giant axon of *Loligo. J. Physiol. (Lond.).* 116:449–472.
2. Verveen, A. A., and L. J. De Felice. 1974. Membrane noise. *Prog. Biophys. Mol. Biol.* 28:189–265.
3. Conti, F., and E. Wanke. 1975. Channel noise in nerve membranes and lipid bilayers. *Q. Rev. Biophys.* 8:451–506.
4. Stevens, C. F. 1977. Study of membrane permeability changes by fluctuation analysis. *Nature (Lond.).* 270:391–396.
5. Lecar, H., and R. Nossal. 1971. Theory of threshold fluctuations in nerves. I. Relationships between electrical noise and fluctuations in axon firing; II. Analysis of various sources of membrane noise. *Biophys. J.* 11:1048–1065, 1068–1084, respectively.
6. Horsthemke, W., and M. Malek-Mansour. 1976. Influence of external noise on nonequilibrium phase transitions. *Z. Physik. B*24:307–313.
7. Horsthemke, W., and R. Lefever. 1977. Phase transition induced by external noise. *Phys. Lett.* 64A:19–21.
8. Lefever, R., and W. Horsthemke. 1979. Bistability in fluctuating environments. Implications in tumor immunology. *Bull. Math. Biol.* 41:469–490.
9. Arnold, L., W. Horsthemke, and R. Lefever. White and coloured external noise and transition phenomena in non-linear systems. Z. Physik. B29:367–373.
10. Lefever, R., and W. Horsthemke. 1979. Multiple transitions induced by light intensity fluctuations in illuminated chemical systems. *Proc. Natl. Acad. Sci. U. S. A.* 76:2490–2494.
11. Kawakubo, R., S. Kabashima, and Y. Tsuchiya. 1978. Experimental studies of some phase transitions in nonequilibrium open systems. *Suppl. Prog. Theoret. Phys.* 64:150–163.
12. Kabashima, S., and T. Kawakubo. 1979. Observation of noise-induced phase transition in a parametric oscillator. *Phys. Lett.* 70A:375–376.
13. Kabashima, S., S. Kogure, T. Kawakubo, and T. Okada. 1979. Oscillatory to nonoscillatory transition due to external noise in a parametric oscillator. *J. Appl. Phys.* 50:6296–6315.
14. De Kepper, P., and W. Horsthemke. 1978. Etude d'une réaction chimique périodique. Influence de la lumière et transitions induites par un bruit externe. *C.R. Acad. Sci. Paris.* 287C:251–254.
15. De Kepper, P., and W. Horsthemke. 1979. Experimental evidence of noise-induced transitions in an open chemical system. In Synergetics. Far from Equilibrium. A. Pacault and C. Vidal, editors. Springer-Verlag, Heidelberg. 61–63.
16. Narahashi, J., J. W. Moore, and W. R. Scott. 1969. TTX blockage of sodium conductance increase in lobster giant axons. *J. Gen. Physiol.* 47:965–974.
17. Tasaki, J., and S. Hagiwara. 1957. Demonstration of two stable potential states in squid giant axon under tetraethylammonium chloride. *J. Gen. Physiol.* 40:851–862.
18. Armstrong, C. M., F. Bezanilla, and E. Rojas. 1973. Destruction of sodium inactivation in squid axons perfused with pronase. *J. Gen. Physiol.* 62:375–391.
19. Pawula, R. F. 1967. Generalizations and extensions of the Fokker-Planck-Kolmogorov equations. *I.E.E.E. Trans. Inf. Theory.* 13:33–45.

20. Pawula, R. F. 1977. The probability density and level-crossing of first-order non-linear systems driven by the random telegraph signal. *Int. J. Control.* 25:283–292.
21. Kitahara, K., W. Horsthemke, and R. Lefever. 1979. Coloured-noise-induced transitions: exact results for external dichotomous markovian noise. *Phys. Lett.* 70A:377–380.
22. De Goede, J., and A. A. Verveen. 1977. Electrical membrane noise: its origin and interpretation. *In* Electrical phenomena at the biological membrane level. E. Roux, editor. Elsevier Scientific Publishing Co., Amsterdam. 337–348.
23. Begenisich, I., and C. F. Stevens. 1975. How many conductance states do potassium channels have? *Biophys. J.* 15:843–846.
24. Sigworth, F. J. 1977. Sodium channels in nerve apparently have two conductance states. *Nature (Lond.).* 270:265–267.
25. van Lamsweerde-Gallez, D., and A. Meessen. 1975. The role of the proteins in a dipole model for steady state ionic transport through biological membranes. *J. Membr. Biol.* 23:103–126.
26. Hill, T. L., and Y. Chen. 1972. On the theory of ion transport across the nerve membrane. VI. Free energy and activation free energies of conformational change. *Proc. Natl. Acad. Sci. U. S. A.* 69:1723–1726.
27. Almeida, S. P., J. D. Bond, and T. C. Ward. 1971. The dipole model and phase transitions in biological membranes. *Biophys. J.* 4:995–1001.
28. Changeux, J. P., J. Thiéry, Y. Tung, and C. Kittel. 1967. On the cooperativity of biological membranes. *Proc. Natl. Acad. Sci. U. S. A.* 57:335–341.
29. Blumenthal, R., J. P. Changeux, and R. Lefever. 1970. Membrane excitability and dissipative instabilities. *J. Membr. Biol.* 2:351–374.
30. Kijima, H., and S. Kijima. 1978. Co-operative response of chemically excitable membrane. *J. Theor. Biol.* 71:567–585.
31. Hill, T. L., and Y. Chen. 1971. On the theory of ion transport across the nerve membrane II. Potassium ion kinetics and cooperativity (with $x = 4$); III. Potassium ion kinetics and cooperativity (with $x = 4, 6, 9$). *Proc. Natl. Acad. Sci. U. S. A.* 68:1711–1715 and 2488–2492, respectively.
32. Horsthemke, W. 1980. Nonequilibrium transitions induced by external white and coloured noise. *In* Dynamics of Synergetic Systems. H. Haken, editor. Springer-Verlag, Heidelberg. p. 67–77.